ELSEVIER

1 February 2000

Optics Communications 174 (2000) 445–453

OPTICS COMMUNICATIONS

www.elsevier.com/locate/optcom

A new method of finding the optical constants of a solid from the reflectance and transmittance spectrograms of its slab

M.A. Khashan *, A.M. El-Naggar

Physics Department, Faculty of Science, Ain Shams University, Cairo, Egypt

Received 1 September 1999; accepted 18 November 1999

Abstract

The reflectance and the transmittance of dielectric (glass) and semiconductor (silicon) slabs are measured and used to calculate, by means of an iteration procedure, the attenuation factor of each sample and the Fresnel reflectance and transmittance of its interface. These three parameters determine the refractive index and the extinction coefficient and their dispersion. The dispersion curves across a wide spectral range, 0.2–3 μm, are used to determine the atomic and quantum constants of both silicon (undoped polycrystalline) and glass (corning). © 2000 Published by Elsevier Science B.V. All rights reserved.

PACS: 78.20.Ci
Keywords: Refractive index; Extinction coefficient; Dispersion; Dielectric; Semiconductor

1. Introduction

The interaction of light radiation with matter yields a great deal of information about the atomic and molecular properties of various substances. In view of this interaction, the light transmission through a medium and the reflection at its boundary interfaces are modified according to the response of the constituent quantum species to the interacting photons. In the present paper, the reflectance and the transmittance of dielectric (glass) and semiconductor (silicon) slabs are used to determine the real and imaginary parts of their complex refractive index, $n - ik$. Considering the incoherent interference of an infinite number of decaying waves between the plane-parallel slab interfaces, we obtain expressions for measurable slab reflectance and transmittance. A new method of data reduction based on a standard iteration process is used to analyze these two parameters. The novel features of the present technique can be outlined as follows. First, the sample absorbance is accurately determined by means of the iteration process in such a way that the slab attenuation and the Fresnel reflectance and transmittance of its interface are separately found. Then, the extinction coefficient is solely determined from the sample attenuation, whereas the refractive index is obtained from a more general formula combining the Fresnel interface reflectance and the extinction coefficient together. In this manner, the anomalous dispersion of n can be defined, for the first time to the authors' knowledge, in a wide spectral range extending from 0.2 to 3 μm wavelength. The importance of finding the anoma-

* Corresponding author. Fax: +20-2-282-2189; e-mail: mkhashan@hotmail.com

PII: S0030-4018(99)00721-X

lous dispersion stems from the fact that many absorption bands can be precisely characterized in both the infrared (IR) and ultraviolet (UV) sides of spectrum. It is also shown below that the steep edge on the long-wavelength side of the k-profile obeys the Fermi–Dirac distribution function so that the Fermi energy can be deduced directly from the experimental data.

2. Slab reflectance and transmittance

Fig. 1 describes how light is reflected and transmitted by a slab of a homogeneous solid material having two plane-parallel faces. The ray scheme in this figure is used to express the slab reflectance, R, and transmittance, T, in terms of the internal and external reflectance, R_s, R'_s, and transmittance T_s and T'_s of the slab interfaces, respectively. When white light reflected and transmitted by the slab is analyzed by a spectrograph, fringes of equal chromatic order (FECOs) [1] are produced across the whole spectrum, which becomes channelled [2] in the form of alternate bright and dark bands. The FECOs are inaccessible to observation whenever their period (spacing) is smaller than the resolution limit and/or the sampling interval of the spectrometer. Expressed in wavelength separation, $\Delta\lambda$, the FECO spacing is calculated as $\Delta\lambda = \lambda^2/2nt$, if the slab has a geometrical thickness t and a refractive index n. Estimating $\Delta\lambda$ for the samples involved below, we find the following. For a silicon slab of $t = 1.085$ mm, $\Delta\lambda$ changes from about 0.002 nm at $\lambda = 0.2$ μm where $n = 10$ to about 0.53 nm at $\lambda = 2$ μm where $n = 3.5$. For a glass slab of $t = 0.920$ mm, $\Delta\lambda$ changes from about 0.014 nm at $\lambda = 0.2$ μm where $n = 1.6$ to about 1.47 nm at $\lambda = 2$ μm where $n = 1.5$. Despite their disappearance, the FECOs very significantly affect the values of R and T. To consider the FECO effect, it is worth recalling that the FECO disappearance is attributed to the fact that the slab thickness becomes much greater than the coherence length [3] of any of the wave trains that interfere inside the slab. Under this condition, an infinite number of multiply reflected wave trains interfere incoherently inside the slab. Therefore, we sum their intensities rather than their amplitudes to obtain the slab reflectance, R, and transmittance, T, in the following forms [4,5]

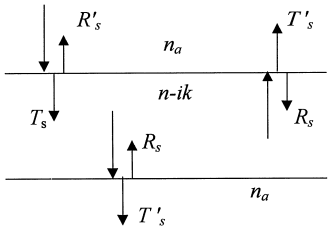

Fig. 1. Ray tracing showing how light is reflected and transmitted at the front and rear interfaces of a slab having a complex refractive index, $n - ik$, in a laboratory atmosphere having a refractive index n_a. The external and internal interface reflectance and transmittance coefficients are differentiated by primes.

$$R = R'_s + R_s \frac{\eta^2 T_s T'_s}{1 - \eta^2 R_s^2} \tag{1}$$

$$T = \eta \frac{T_s T'_s}{1 - \eta^2 R_s^2}. \tag{2}$$

The attenuation factor, η, appearing in these expressions, plays an important role for it measures the absorption coefficient, α, of a slab material having a complex refractive index, $n - ik$. According to Lambert's absorption law [6], the attenuation factor, η, is defined as

$$\eta = \exp(-\alpha t) \tag{3}$$

for a slab having a geometrical thickness, t, and an absorption coefficient $\alpha = 4\pi k/\lambda$ with λ being the wavelength of the incident probe photon in free space. The present paper is mainly intended to determine η from the measured slab R and T. Unfortunately, Eqs. (1) and (2) cannot be solved for η since they contain the unknown interface reflectance and transmittance. These latter parameters depend on the refractive index, n, and the extinction coefficient, k, according to the Fresnel formulae for normal incidence (see Refs. [7,8] for example)

$$R_s = R'_s = \frac{(n - n_a)^2 + k^2}{(n + n_a)^2 + k^2} \tag{4}$$

$$T_s = T'_s = \frac{4n_a\sqrt{n^2 + k^2}}{(n + n_a)^2 + k^2} \tag{5}$$

where n_a is the refractive index of the laboratory atmosphere (air) in which the slab parameters are

measurable. Taking the last two expressions into account, combining Eqs. (1) and (2), and solving for the interface reflectance and transmittance, we get

$$R_s = \frac{R}{1+\eta T} \tag{6}$$

$$T_s = \sqrt{\left(1-\eta^2 R_s^2\right)T/\eta}\,. \tag{7}$$

A close inspection of these two equations shows that we are confronted with a serious problem since their right-hand sides are not free from the unknown parameters η. To tackle this problem we adopt below a procedure of data reduction based on an iteration technique, which enables the interface coefficients, R_s and T_s, and the attenuation factor, η, of the medium to be found. Our approach is based on the frequent application of the conservation law [9]

$$R_s + T_s + A_t = 1, \tag{8}$$

with the absorbance, A_t, being a measure for the deviation of the sum of reflectance and transmittance from unity. The knowledge of A_t leads to the knowledge of η. To show how η is related to A_t, we draw attention to Lambert's absorption law

$$I = I_0 \exp(-\alpha z)\,. \tag{9}$$

This law describes, in its differential form, how a relative intensity, $\mathrm{d}I/I = -\alpha\,\mathrm{d}z$, is regularly lost every time when light crosses inside the medium equal incremental pathlengths, $\mathrm{d}z$. The depth, z, inside the sample is measured perpendicularly from its front interface where $I = I_0$. By definition [10], the absorbance $A_t = -(\int_0^t \mathrm{d}I)/I_0$, across a thickness, t, of a dissipating medium. Keeping this definition in mind, we find from Eqs. (9) and (3) by integration that

$$A_t = 1 - \eta. \tag{10}$$

In this way, η can be determined, if A_t is known. The latter is simply determined from the equality $A_t = 1 - (R_s + T_s)$, provided that R_s and T_s are known either roughly or precisely. This point is discussed below in more detail.

3. Experimental measurements

In the present work, the reflectance and the transmittance of two samples are used to determine their optical constants. Corning glass is used as a typical dielectric sample whereas undoped polycrystalline silicon is used as a typical intrinsic semiconductor sample. Each sample was prepared in the form of a slab having plane-parallel faces. The slab faces were tested for flatness and parallelism interferometrically without the use of any coating. Reflection two-beam interference was observed directly with the glass slab, but in the case of silicon a master optical glass flat was used in front of silicon faces polished for mirror (specular) reflection. Monochromatic light from a sodium lamp ($\lambda = 589.3$ nm) was used for such tests since its coherence length of about 65 mm was much greater than a slab thickness of about one mm (for each sample). Under this condition high-visibility [3] fringes of equal inclination [11,12] were observed as long as the slab interfaces were plane and parallel. The Fizeau fringes of equal thickness [11,12] were used with He–Ne laser wavelength $\lambda = 632.8$ nm to detect any local deviation from surface flatness. Surface defects less than $\lambda/10$ were detectable especially with the aid of dark fringes. This test was performed across working areas of 9.2×15.9 mm^2 for Si, and 10×10 mm^2 for glass. Our glass sample was corning type 7059 having a geometrical thickness of 0.920 ± 0.002 mm. Our Si sample of 1.085 ± 0.002 mm thickness was cut from an undoped polycrystalline silicon rod of high purity supplied by Wacker-Chemitronic. This Si sample was reported by the manufacturer to have a donor level greater than 600 Ω cm and an acceptor level greater than 3000 Ω cm.

The reflectance, R, and the transmittance, T, of each slab was measured to accuracy of 0.003 by means of a computer-aided two-beam spectrophotometer (Shimadzu-3101PC UV–VIS–NIR) having a resolution limit of 0.2 nm and a sampling interval of 2 nm. Our measurements were carried out at 24°C temperature for the spectral range 0.2–3 μm with the incident beam making an angle of $5.0 \pm 0.1°$ to the normal to the slab (external) faces. With such a small incidence angle Eqs. (1)–(7) derived for normal incidence are applicable specially if we recall that the refraction angle becomes smaller than 5 degrees inside the slab.

The results of our measurement are reproduced in Fig. 2 for glass, and in Fig. 3 for silicon. We note in Fig. 2 that T of the glass slab shows at both its

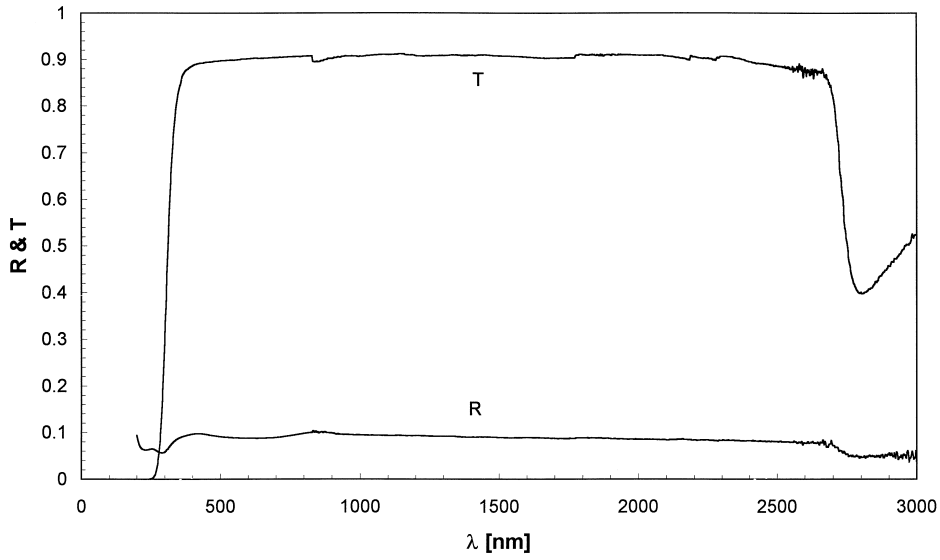

Fig. 2. Measured reflectance, *R*, and transmittance, *T*, of a corning glass slab having a thickness of 0.92 mm at 24°C.

extreme ends two steep depressions. At the same positions, the reflectance, *R*, of the same glass slab exhibits two shallow depressions. This behavior indicates the existence of two strong absorption bands for glass in both the IR and UV ends of spectrum. This conclusion will be confirmed below more quantitatively. In Fig. 3, *T* of the Si slab shows abrupt depressions in both the near IR and the UV sides of

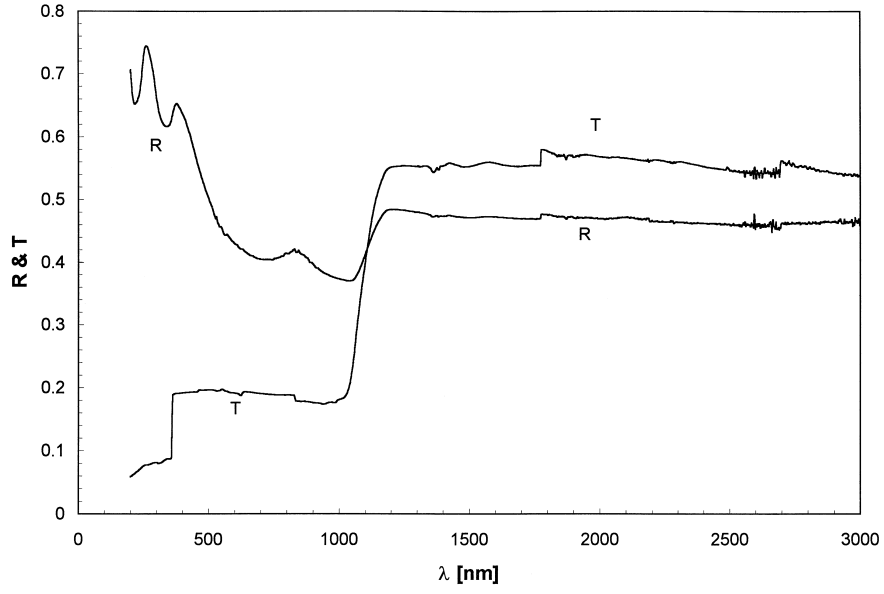

Fig. 3. Measured reflectance, *R*, and transmittance, *T*, of undoped polycrystalline Si slab having a thickness of 1.085 mm at 24°C.

the spectrum. At the same region of spectrum, R of the Si slab steadily increases while it is exhibiting a few narrow ripples indicating the existence of a couple of sharp absorption bands overlapping a broad conduction band characteristic for semiconductor materials [13,14]. The conduction band of Si is investigated below in more detail.

4. Method of data reduction

The present work is mainly aiming at using the spectral functions $R(\lambda)$ and $T(\lambda)$ of the slabs in Figs. 2 and 3 to find the sample attenuation factor, $\eta(\lambda)$, and the interface reflectance, $R_s(\lambda)$ and transmittance, $T_s(\lambda)$. These three parameters lead to the knowledge of the real and imaginary parts of $n - ik$ separately and their dispersion. This can be accomplished by means of an iteration procedure consisting of the following steps. In the first step, we assume as a first approximation that $\eta = 1$. Then, we use Eqs. (6) and (7) to get rough values for R_s and T_s. These values are used in a second step to calculate from Eq. (8) a rough value for A_t, which yields via Eq. (10) a rough value for η. This η-value is used, in a third step, to calculate from Eqs. (6) and (7) new R_s and T_s values, which are used in their turn to find a new value for η as before. This step is repeated many times until a stationary function $A_t(\lambda)$ do not change its values appreciably as new η-values are substituted in Eqs. (6) and (7) The stationary solution can be easily discovered by plotting A_t versus λ for all the preceding steps as shown in Fig. 4 (for Si, specifically). These plots show that the curves $A_t(\lambda)$ oscillate about a stationary solution which seems to be approached asymptotically. From a practical viewpoint, the stationary function $A_t(\lambda)$ is obtained when the repetition of the calculations does not lead to A_t-values differing from each other by values greater than 0.004. This limit is calculated from Eq. (8) as the error of A_t, which corresponds to the error 0.003 of measuring either R or T by the spectrophotometer at hand. We found that six oscillations led to a stationary solution for Si, but in the case of glass, only two trials led to its stationary function, $A_t(\lambda)$. The final step is to test the correctness of the stationary solution $A_t(\lambda)$ by using the corresponding $\eta(\lambda)$, $R_s(\lambda)$ and $T_s(\lambda)$ to simulate by the aid of Eqs. (1) and (2) the experimentally measured $R(\lambda)$ and $T(\lambda)$ of each slab. It is interesting to note that this simulation was astonishingly perfect because the cal-

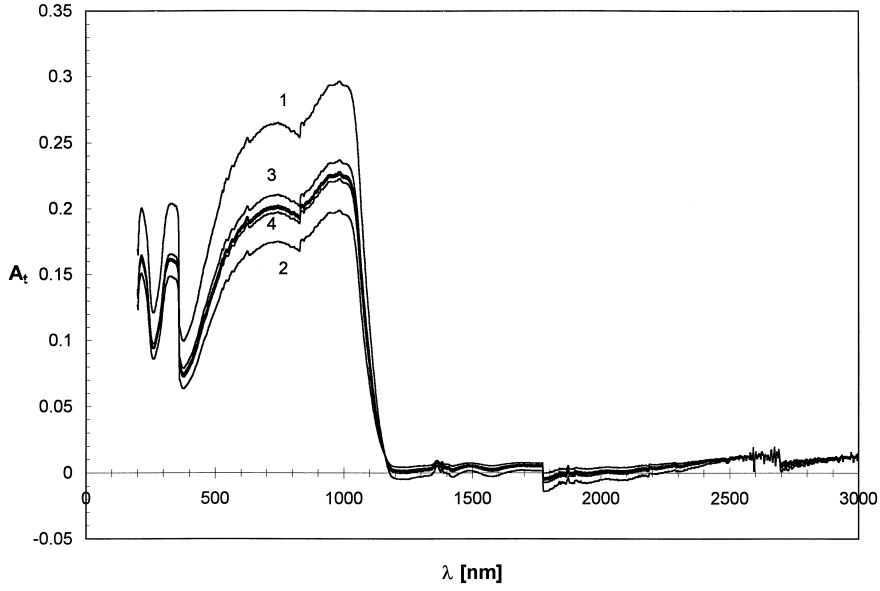

Fig. 4. Search for the correct absorbance, A_t, of a Si slab. The degree of accuracy increases from lower to higher numbers that are written past each curve.

culated and the experimental values of $R(\lambda)$ and $T(\lambda)$ are excellently coincident for 1401 experimental points within the experimental error 0.003 of either R or T.

5. Determination of optical constants

The knowledge of η enables the extinction coefficient, k, to be determined from the expression

$$k = -(\lambda/4\pi t)\ln\eta. \tag{11}$$

The relative error of k is estimated by means of this expression

$$\frac{\delta k}{k} = \sqrt{\left(\frac{\delta\eta}{\eta\ln\eta}\right)^2 + \left(\frac{\delta\lambda}{\lambda}\right)^2 + \left(\frac{\delta t}{t}\right)^2} \tag{12}$$

which follows from Eq. (11) by differentiation, assuming that π is a constant and the differentials $\delta\eta$, $\delta\lambda$, and δt stand for the errors of η, λ and t, respectively.

The interface reflectance R_s can be used to determine the refractive index, n, of the slab material since the Fresnel Eq. (4) is solved for n to get this general equation

$$n = n_a\left[\frac{1+R_s}{1-R_s} + \sqrt{\frac{4R_s}{(1-R_s)^2} - \frac{k^2}{n_a^2}}\right]. \tag{13}$$

The refractive index has its absolute error, δn, estimated by this equation

$$\delta n = \sqrt{\left(\frac{\partial n}{\partial n_a}\delta n_a\right)^2 + \left(\frac{\partial n}{\partial R_s}\delta R_s\right)^2 + \left(\frac{\partial n}{\partial k}\delta k\right)^2} \tag{14}$$

where δn_a, δR_s and δk are the experimental errors, and the partial derivatives are determined from Eq. (13). The results of using Eqs. (11) and (13) to find the optical constants for glass and silicon are plotted versus wavelength in Figs. 5 and 6, respectively.

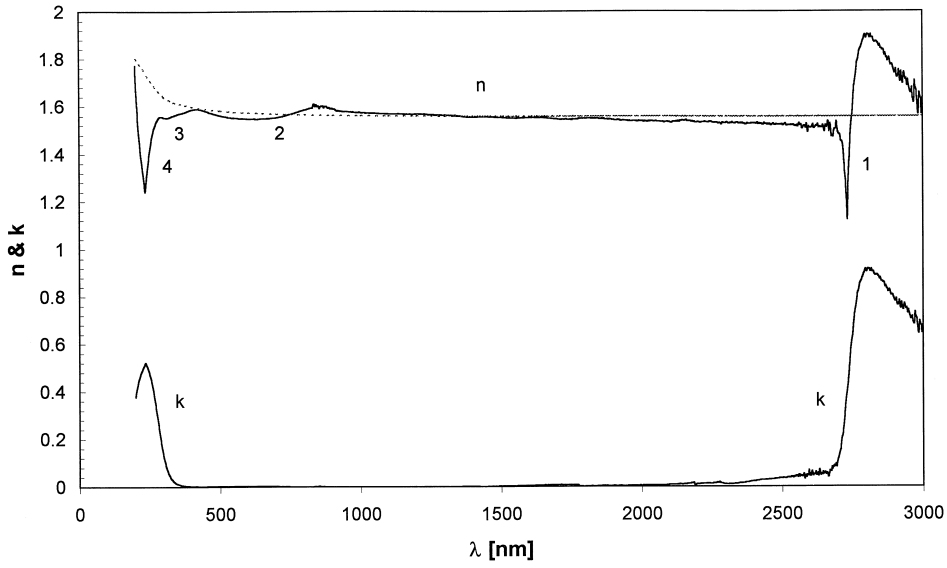

Fig. 5. Experimentally measured dispersion (continuous curves) of the real and imaginary parts of the glass complex refractive index, $n - ik$. The numbers indicate anomalous-dispersion branches corresponding to k-bands. The Cauchy dispersion function, which fits the normal-dispersion parts, is represented by a dotted curve.

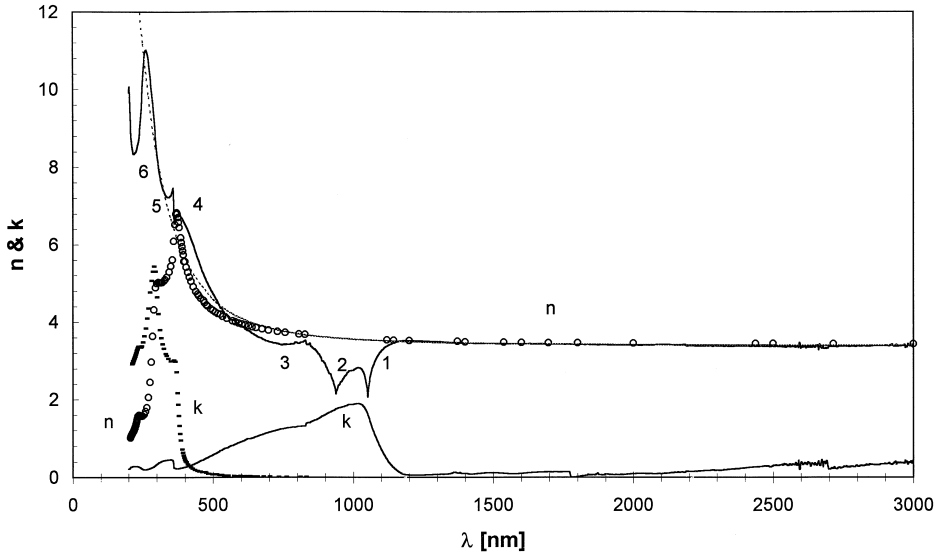

Fig. 6. Experimentally measured dispersion (continuous curves) of the real and imaginary parts of Si complex refractive index, $n - \mathrm{i}k$. The numbers indicate anomalous-dispersion branches corresponding to partially overlapping k-bands. The Cauchy dispersion function, which fits the normal-dispersion parts, is represented by a dotted curve. The n- and k-values of other authors are represented by circles and dashes, respectively.

These results are obtained assuming that $n_a = 1$ with an error $\delta n_a = 3 \times 10^{-4}$, and Eqs. (12) and (14) are used to estimate errors $\delta k/k = 0.005$ and $\delta n = 0.007$.

6. Dispersion and quantum parameters of solids

The interaction of electromagnetic waves with matter is responsible for the variation of the wave speed with wavelength according to the dispersion function [15–17]

$$n^2 = 1 + \sum_{j=i+1}^{\infty} a_{ij} \frac{\left(\frac{\lambda}{\lambda_{ij}}\right)^2 - 1}{\left(\frac{\lambda}{\lambda_{ik}} - \frac{\lambda_{ij}}{\lambda}\right)^2 + \frac{1}{Q_{ij}^2}}. \qquad (15)$$

In this expression, we use the following atomic parameters

$$a_{ij} = r_e N f_{ij} \lambda_{ij}^2 / 2\pi \qquad (16)$$

$$r_e = e^2/mc^2 \qquad (17)$$

$$Q_{ij} = \lambda_{ij}/\delta\lambda_{ij}. \qquad (18)$$

These parameters have the following physical meanings. $r_e = 2.818 \times 10^{-13}$ cm is the classical radius of an electron having a charge, e, and a mass, m, and experiencing a transition from a lower energy level, i, to a higher energy level, j, when it absorbs a photon associated with a (transition) wavelength λ_{ij}. The atomic number density N determines the population of the ground level, i. The oscillator strength, f_{ij}, is a fraction of N, which takes part in a given $i \to j$ transition. The light speed in free space is denoted as c. Q_{ij} is the quality factor of the quantum oscillator whose resonance (or absorption) band has a peak wavelength λ_{ij} and a half-width $\delta\lambda_{ij}$. It is interesting to note that both a_{ij} and Q_{ij} determine a maximum value, $n_{max} = (1 + a_{ij}Q_{ij}/2)^{1/2}$ and a minimum value, $n_{min} = (1 - a_{ij}Q_{ij}/2)^{1/2}$, of the refractive index, n, at the top and the bottom of each anomalous-dispersion branch where $\lambda = \lambda_{ij} \pm \delta\lambda_{ij}$, respectively. The dispersion curve of glass in Fig. 5 is noted to have 4 anomalous-dispersion branches: two of which are deep (at IR and UV ends) and two are shallow (closely to the UV band). The corresponding transition wavelengths are $\lambda_{ij} = 2763$, 721, 358, 261 nm. Similarly, the dispersion curve of Si in Fig. 6 has 6 anomalous-dispersion branches corre-

sponding to transition wavelengths $\lambda_{ij} = 1050$, 978, 779, 368, 346, and 233 nm. It is worth mentioning that these wavelengths could not be deduced from the function $k(\lambda)$ of Si unless a tedious process of deconvolution were adopted since this function is the resultant of a number of partially overlapping broad Lorenzian profiles. The portions of the dispersion curve in-between the anomalous-dispersion branches are known to represent a normal dispersion, which obey, as a good approximation, the Cauchy dispersion equation

$$n^2 = A + B/\lambda^2 + C/\lambda^4 + \ldots. \tag{19}$$

This function is derived from Eq. (15), assuming that Q_{ij} tends to infinity and the resulting Sellmeier function

$$n^2 = 1 + \sum_{j=i+1}^{\infty} \frac{a_{ij}}{1 - \left(\lambda_{ij}/\lambda\right)^2} \tag{20}$$

is replaced by the McLaurin expansion. In this way, the Cauchy coefficients A, B and C are defined as

$$A = 1 + \sum_{j=i+1}^{\infty} a_{ij}, \quad B = \sum_{j=i+1}^{\infty} a_{ij}\lambda_{ij}^2,$$

$$C = \sum_{j=i+1}^{\infty} a_{ij}\lambda_{ij}^4. \tag{21}$$

We found Cauchy coefficients: $A = 2.417$, $B = 1.979 \times 10^4$ nm^2 and $C = 5.174 \times 10^8$ nm^4 for glass and $A = 11.402$, $B = 8.582 \times 10^5$ nm^2 and $C = 3.883 \times 10^{11}$ nm^4 for Si. The Cauchy functions in these cases are represented in Figs. 5 and 6 by dotted curves.

There remains one more interesting point. It is noted that the functions $k(\lambda)$ for both Si and glass have steep edges toward the IR side of spectrum. These edges are fitted to the Fermi–Dirac distribution function

$$F(\lambda) = \frac{1}{1 + \exp\left(\dfrac{E_F - E}{k_B T}\right)} \tag{22}$$

where E_F is the Fermi energy, $E = hc/\lambda$ is the variable photon energy, and $k_B T$ is the thermal energy at the moment of measuring the sample spectrum. Here, h is the Planck constant, k_B is the Boltzman constant, and T is the absolute temperature. We found $E_F = 1.139$ eV for Si and $E_F = 4.350$ eV for glass.

For the sake of comparison with the results of other authors, we reproduce in Fig. 6 experimental data (mainly Ref. [18]) for Si compiled in Ref. [19] from various works (circles for n, and dashes for k). The agreement with our n-data is remarkable in the region of normal dispersion up to $\lambda = 371$ nm, and the Cauchy formula is the same for all data. There is also a similarity between the k-profiles in Fig. 6 because their long-wavelength sides obey the Fermi–Dirac function (22) but a higher Fermi energy $E_F = 3.399$ eV is calculated from the data of the other authors. In general, a significant displacement is noted between the peaks of the k-profiles. This displacement may be attributed to the fact that our sample had a resistivity higher than those of the samples of the other authors, which ranged from 10 Ω cm [20–22] to 1000 Ω cm [23]. Our experimental data for glass are consistent also with those of other authors [24] but the present work may be considered as the first one that calculates a Fermi energy for glass.

7. Conclusion

Taking incoherent interference into consideration, we adopt an iteration procedure to analyze the measurable reflectance and transmittance of glass and silicon slabs having plane-parallel faces with one-mm thickness. The decay factor is used to determine the extinction coefficient and the Fresnel interface reflectance is used to deduce the refractive index. The dispersion of these two optical constants is used to find the transition wavelengths and the Fermi energies.

References

[1] S. Tolansky, Multiple-Beam Interferometry of Surfaces and Films, Dover, New York, 1970, Chapter 8, p. 96.
[2] R.W. Ditchburn, Light, Blackie, London, 1963, Chapter 5, pp. 144–146.
[3] R.W. Ditchburn, Light, Blackie, London, 1963, Chapter 4, p. 79.
[4] R.F. Potter, Basic Parameters for Measuring Optical Proper-

ties, in: E.D. Palik (Ed.), Handbook of Optical Constants of Solids, Academic, Orlando, 1985, p. 25.
[5] G. Kurtüm, Reflectance Spectroscopy: Principles, Methods, Applications, Springer-Verlag, Berlin, 1969, Chapter 4, p. 124.
[6] G. Kurtüm, Reflectance Spectroscopy: Principles, Methods, Applications, Springer-Verlag, Berlin, 1969, Chapter 2, p. 21.
[7] A.V. Sokolov, Optical Properties of Metals, Elsevier, New York, 1967, Chapter 1.
[8] L. Ward, The Optical Constants of Bulk Materials and Films, 2nd edn., Institute of Physics Publishing, Bristol, 1994, Chapter 1, p. 8.
[9] R.F. Potter, Basic Parameters for Measuring Optical Properties, in: E.D. Palik (Ed.), Handbook of Optical Constants of Solids, Academic, Orlando, 1985, p. 18.
[10] P.A. Temple, Thin-film absorptance measurements using laser calorimetry, in: E.D. Palik (Ed.), Handbook of Optical Constants of Solids, Academic, Orlando, 1985, Chapter 7, p. 139.
[11] M.V.R.K. Murty, Newton, Fizeau and Haidinger Interferometers, in: D. Malacara (Ed.), Optical Shop Testing, John Wiley, New York, 1978, Chapter 1, pp. 1–45.
[12] C. Candler, Modern Interferometers, Hilger and Watts, Glasgow, 1951, Chapter 4.
[13] C.F. Klingshirn, Semiconductor Optics, Springer-Verlag, Berlin, 1995, Chapter 10, p. 125.
[14] T.E. Jenkins. Semiconductor Science: Growth and Characterization Techniques, Prentice Hall, New York, 1995, Chapter 5, p. 284.
[15] R.W. Ditchburn, Light, Blackie, London, 1963, Chapter 15, p. 566.
[16] A. Sommerfeld, Optics, Academic, New York, 1967, p. 98.
[17] M. Born, E. Wolf, Principles of Optics, Pergamon, Oxford, 1973, p. 93.
[18] D.E. Aspnes, J.B. Theeten, J. Electrochem. Soc. 127 (1980) 1359.
[19] D.F. Edwards, Silicon (Si), in: E.D. Palik (Ed.), Handbook of Optical Constants of Solids, Academic, Orlando, 1985, pp. 547–569.
[20] D.D. Honijk, W.F. Passchier, M. Mandel, M.N. Afsar, Infrared Phys. 17 (1977) 9.
[21] W.F. Passchier, D.D. Honijk, M. Mandel, M.N. Afsar, J. Phys. D 10 (1977) 509.
[22] J.R. Birch, Infrared Phys. 18 (1978) 613.
[23] M.N. Afsar, J.B. Hasted, Infrared Phys. 18 (1978) 835.
[24] T.S. Izumitani, Optical Glass, American Institute of Physics, New York, 1986, pp. 25–36.